Supplementary Materials: Bimetallic Metal-Organic Framework mediated Synthesis of Ni-Co Catalysts for the Dry Reforming of Methane

Il Son Khan, Adrian Ramirez *, Genrikh Shterk, Luis Garzón-Tovar and Jorge Gascon *

Advanced Catalytic Materials, KAUST Catalysis Center (KCC), King Abdullah University of Science and Technology, Thuwal 23955, Saudi Arabia; ilson.khan@kaust.edu.sa (I.S.K.); genrikh.shterk@kaust.edu.sa (G.S.); luis.garzontovar@kaust.edu.sa (L.G.-T.)

* Correspondence: adrian.galilea@kaust.edu.sa (A.R.); jorge.gascon@kaust.edu.sa (J.G.)

a)

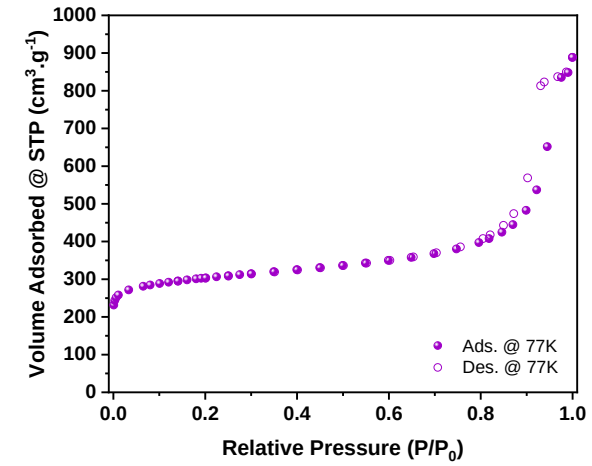

b)

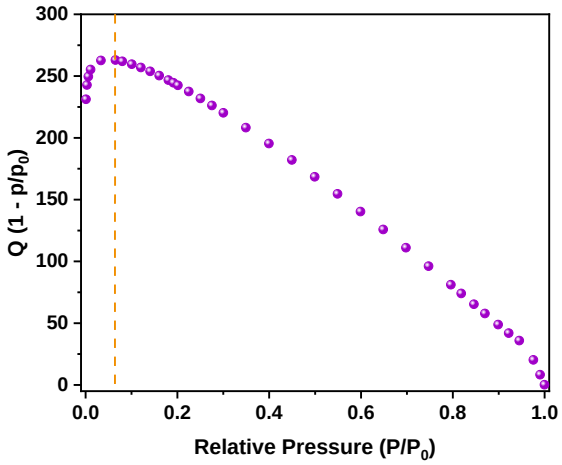

c)

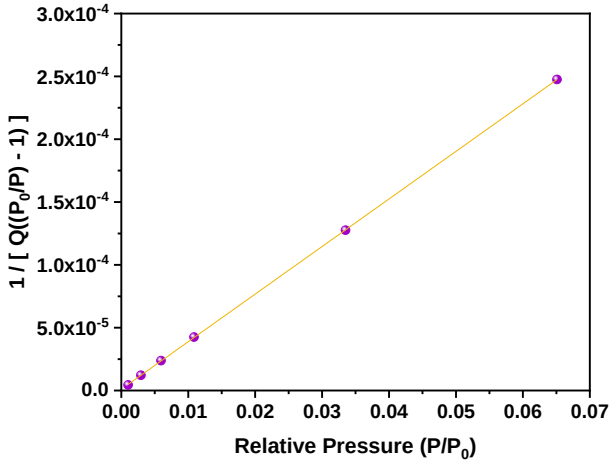

BET Surface area: 1149.2453 ± 2.0268 m^2/g

Slope: 0.003786 ± 0.000007 g/cm^3 STP

Y-intercept: 0.000001 ± 0.000000 g/cm^3 STP

Correlation coefficient: 0.9999938

C constant: 3768.853

Qm: 264.0378 cm^3/g STP

Molecular cross sectional area: 0.1620 nm^2

Figure S1. a) N_2 adsorption isotherm at 77 K, b) Rouquerol plot and c) Brunauer-Emmett-Teller (BET) fit for Ni-MOF-74.

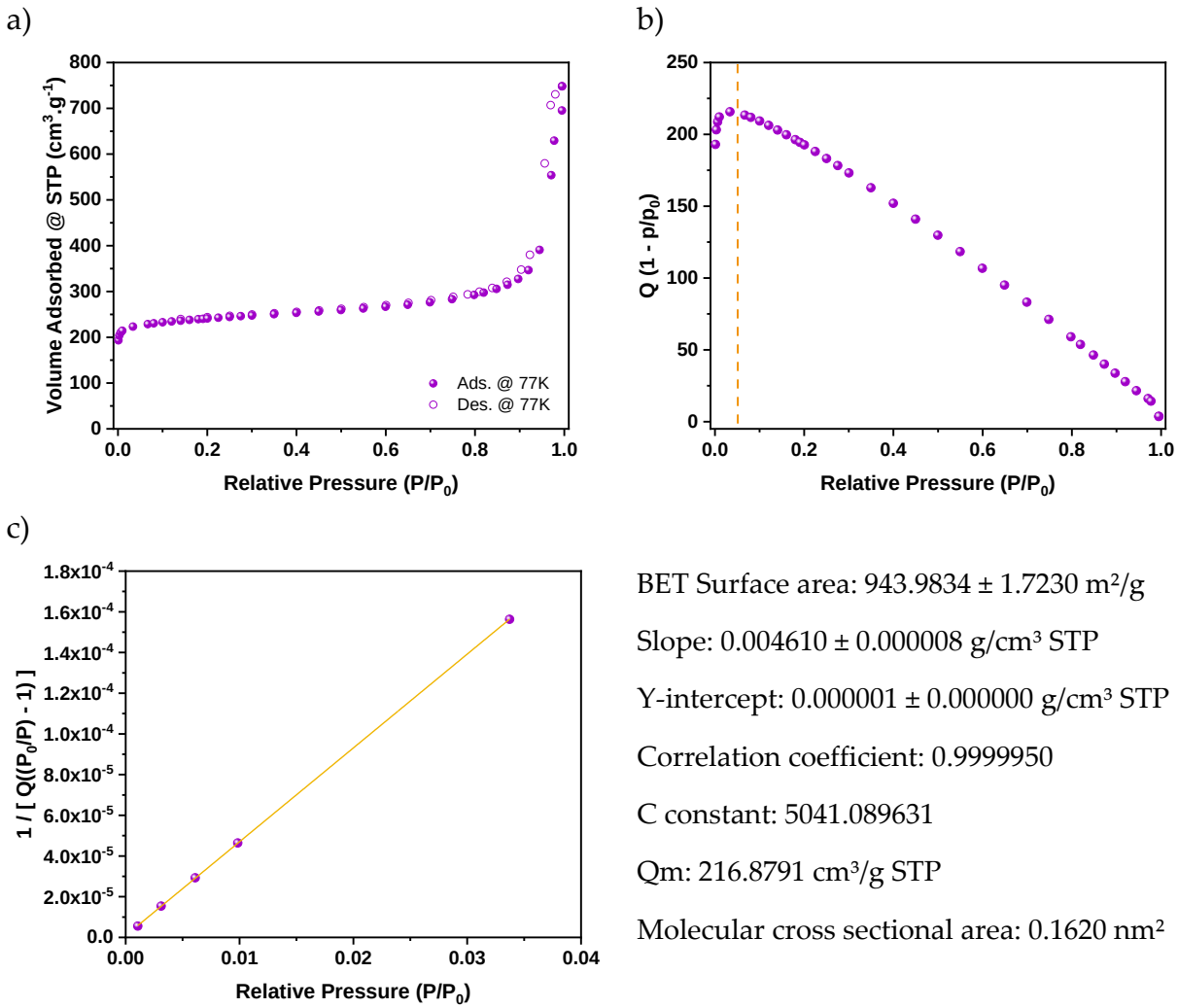

Figure S2. a) N_2 adsorption isotherm at 77 K, b) Rouquerol plot and c) Brunauer-Emmett-Teller (BET) fit for Co-MOF-74.

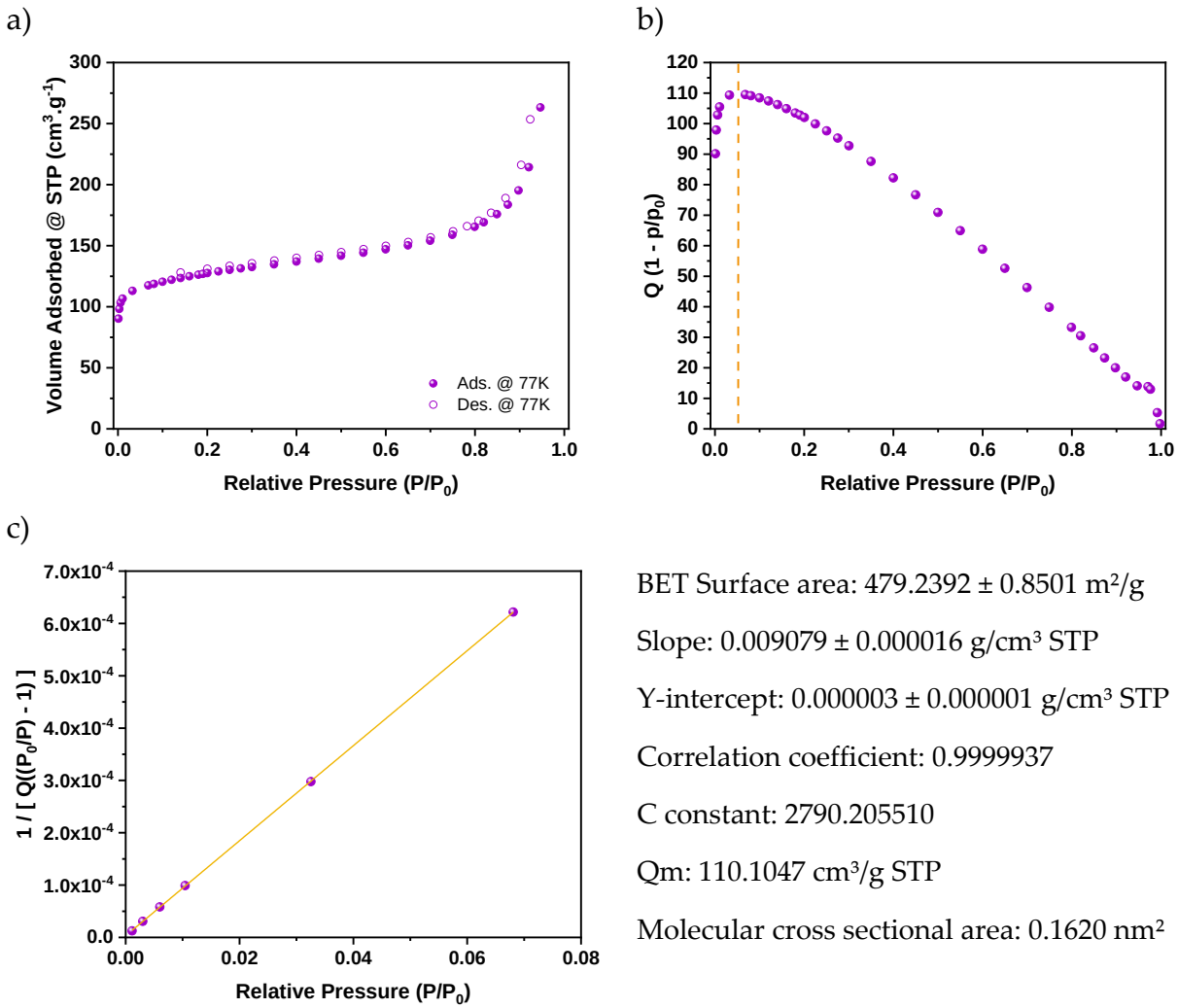

Figure S3. a) N_2 adsorption isotherm at 77 K, b) Rouquerol plot and c) Brunauer-Emmett-Teller (BET) fit for Ni-Co-MOF-74.

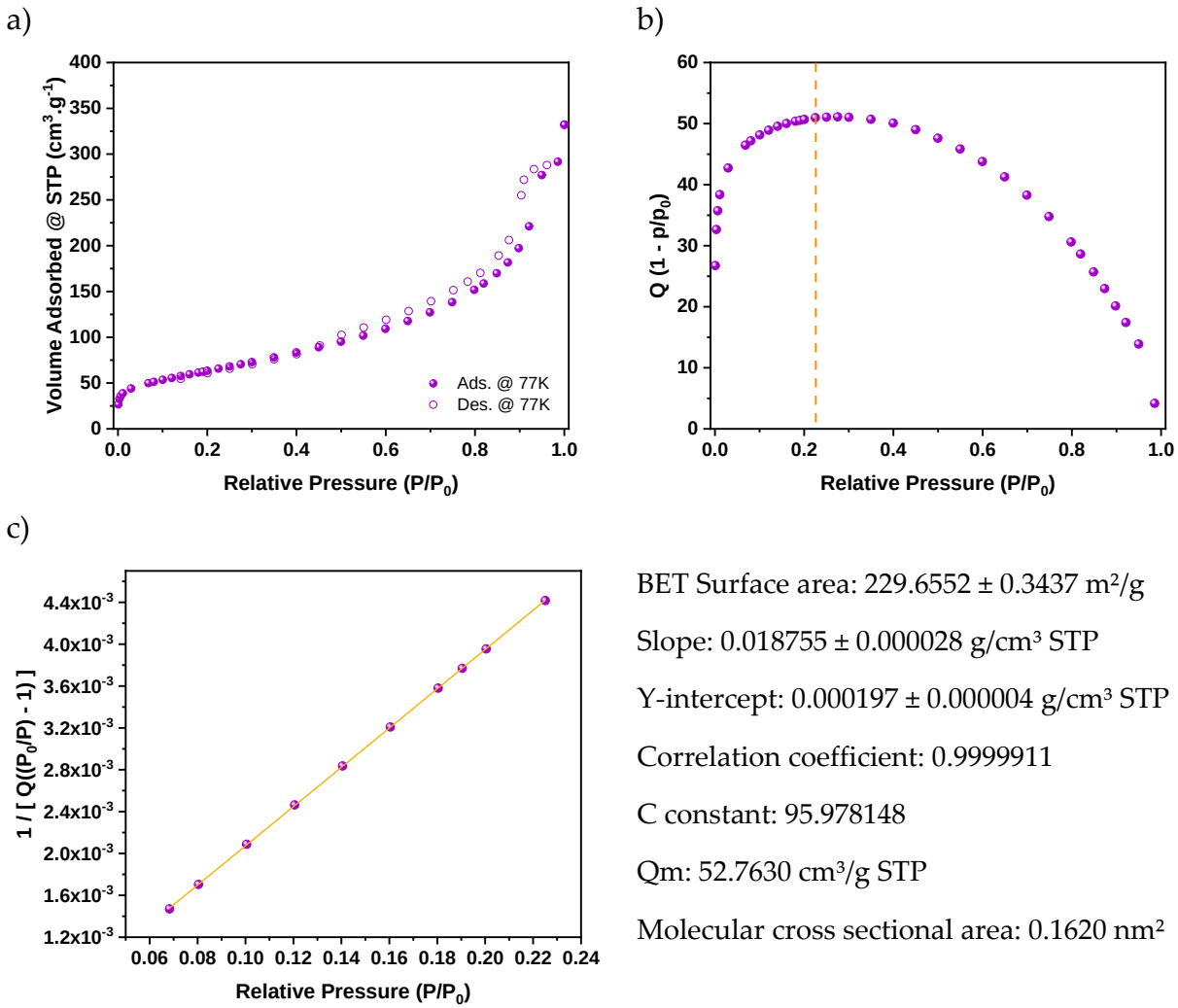

Figure S4. a) N_2 adsorption isotherm at 77 K, b) Rouquerol plot and c) Brunauer-Emmett-Teller (BET) fit for Ni@CMOF-74.

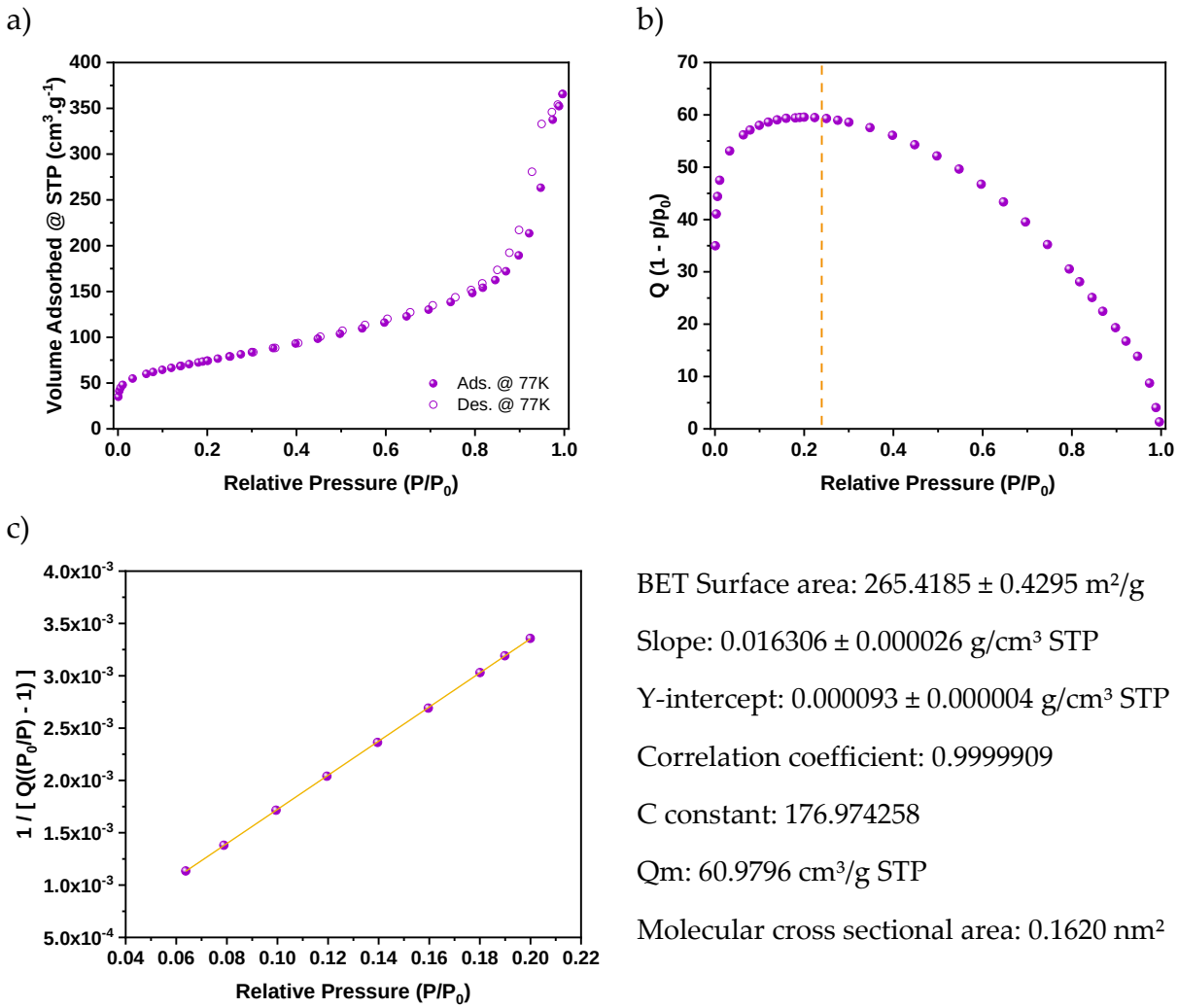

Figure S5. a) N_2 adsorption isotherm at 77 K, b) Rouquerol plot and c) Brunauer-Emmett-Teller (BET) fit for Co@CMOF-74.

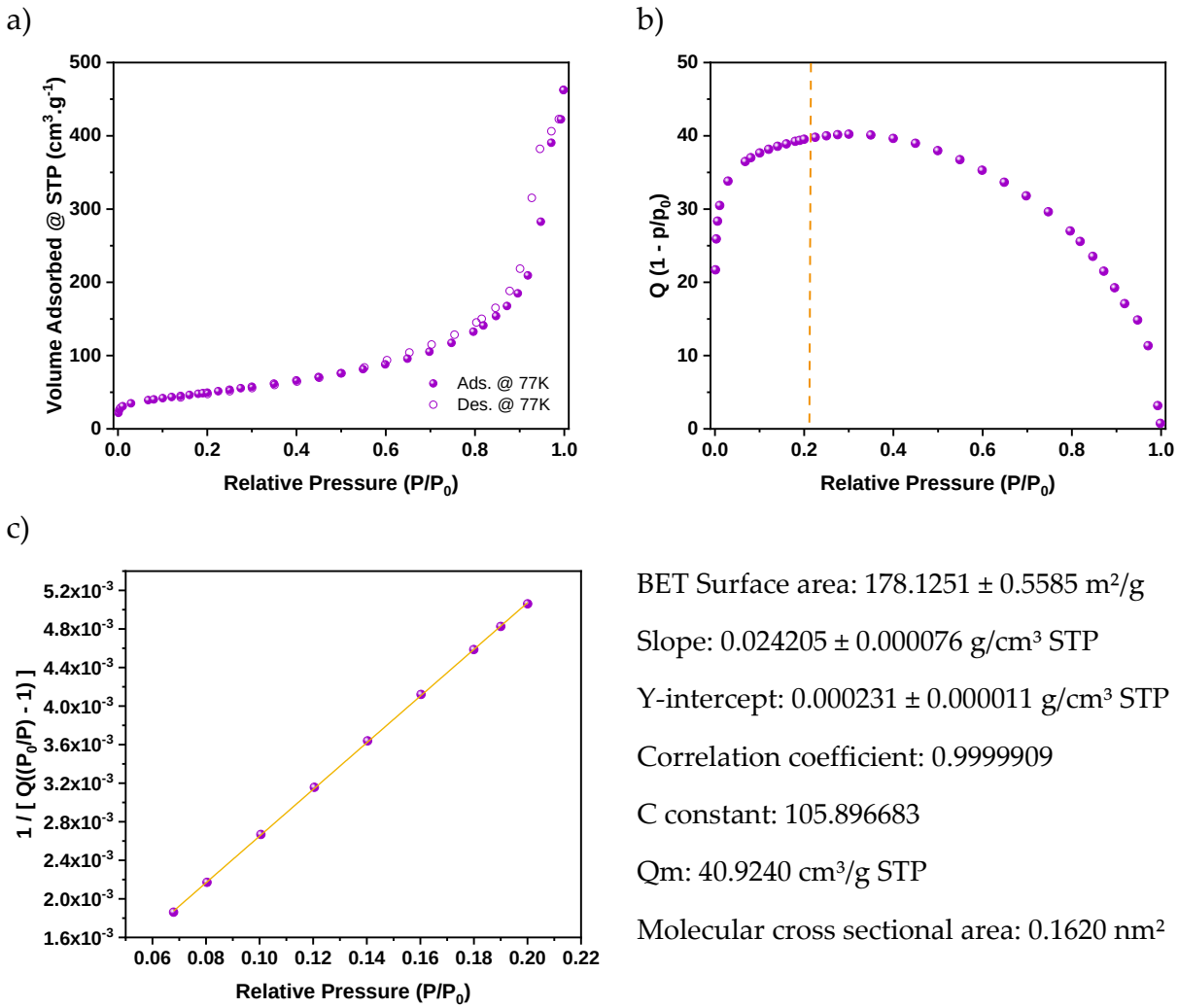

Figure S6. a) N_2 adsorption isotherm at 77 K, b) Rouquerol plot and c) Brunauer-Emmett-Teller (BET) fit for Ni-Co@MOF-74.

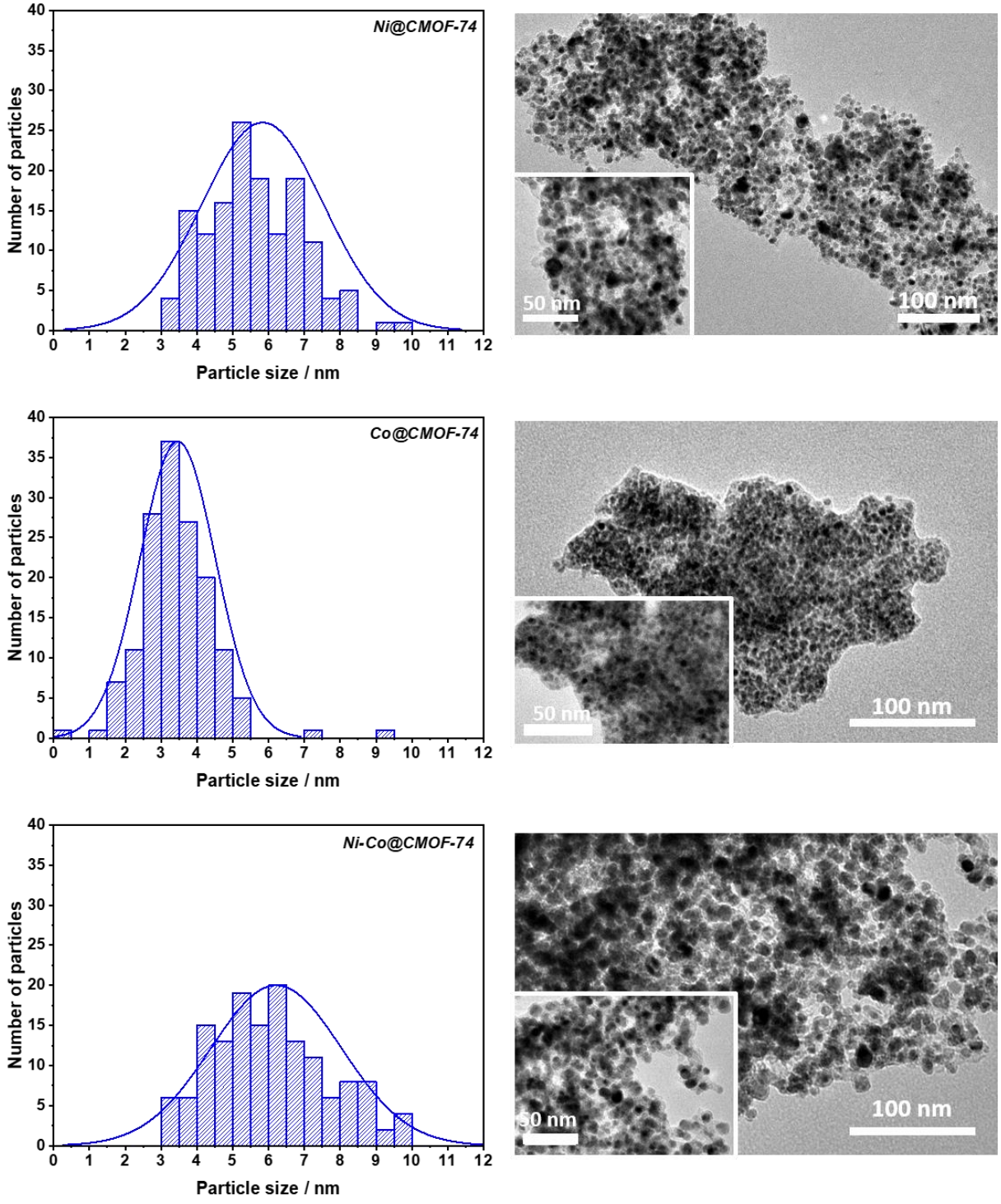

Figure S7. TEM images and MNP size distribution of the different M@CMOF-74 catalysts.

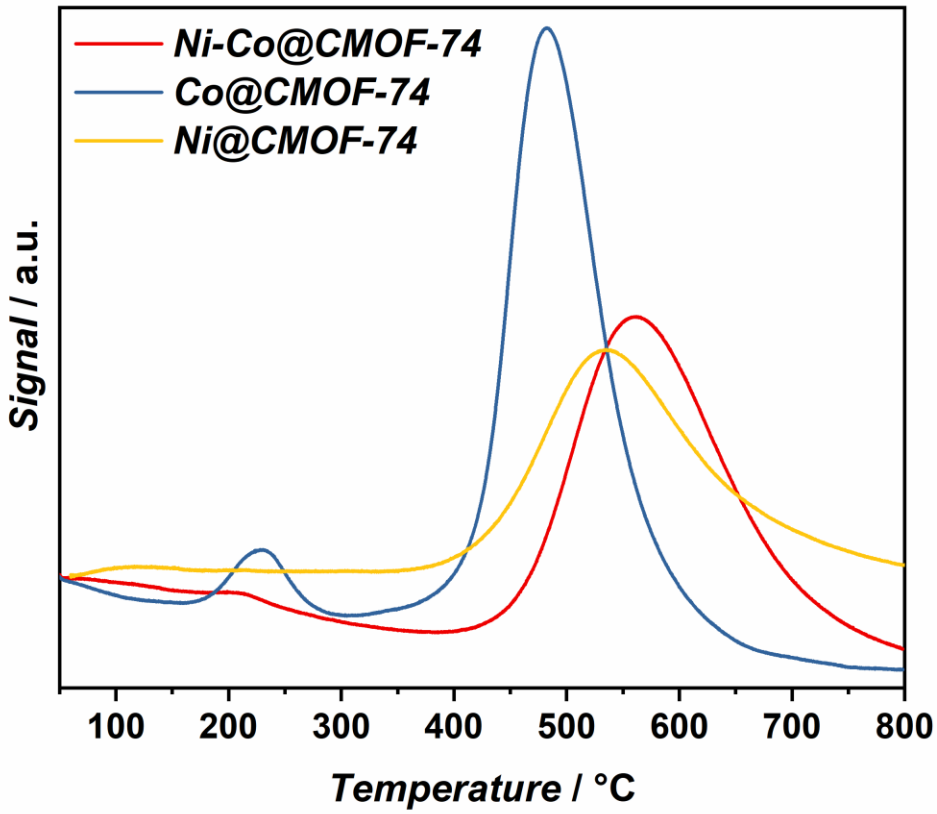

Figure S8. Temperature programed reduction (TPR) profiles of the different M@CMOF-74 catalysts.

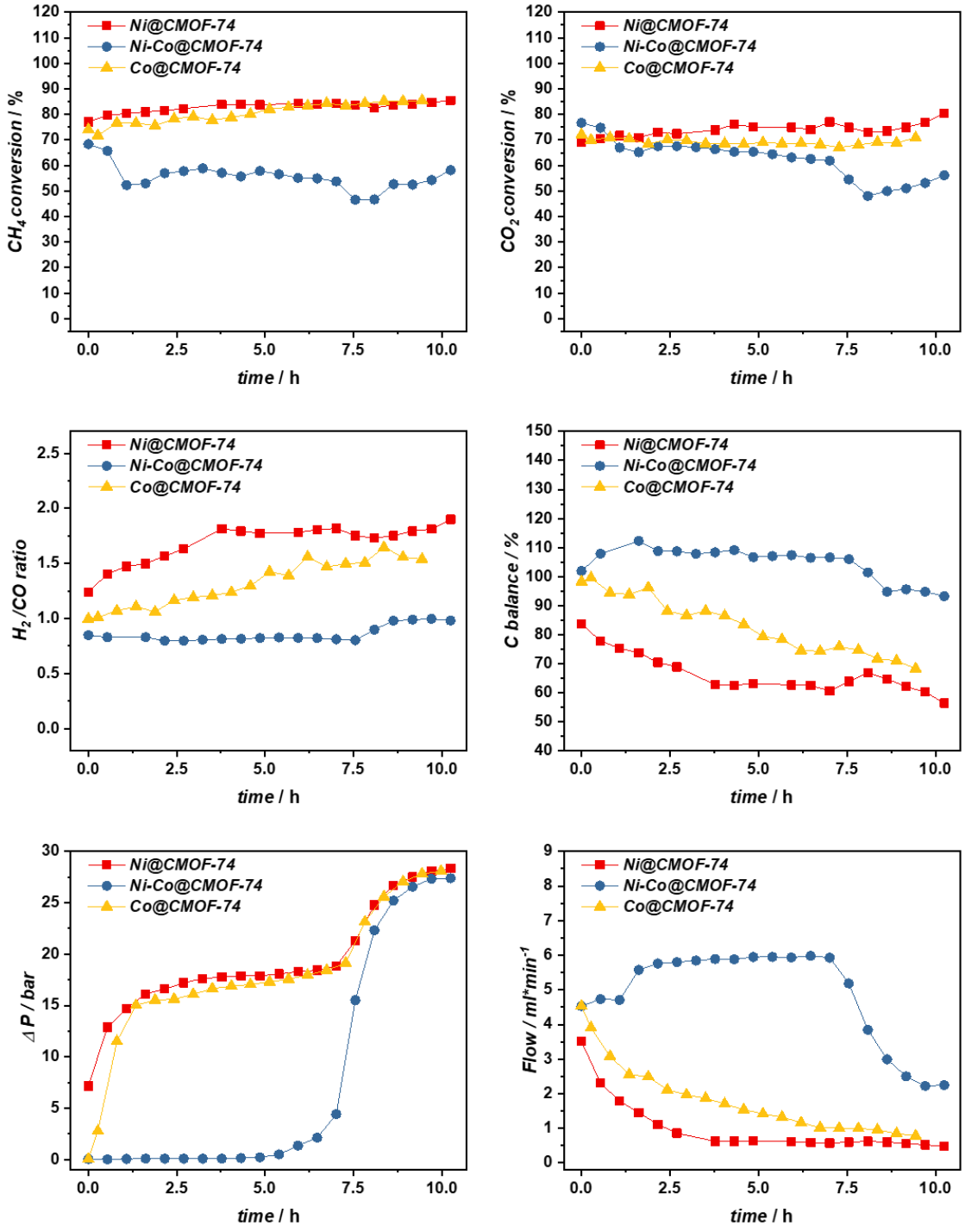

Figure S9. Catalytic results of the different M@CMOF-74 catalysts at 750 °C, 5 bar, 33 $L*h^{-1}*g^{-1}$.

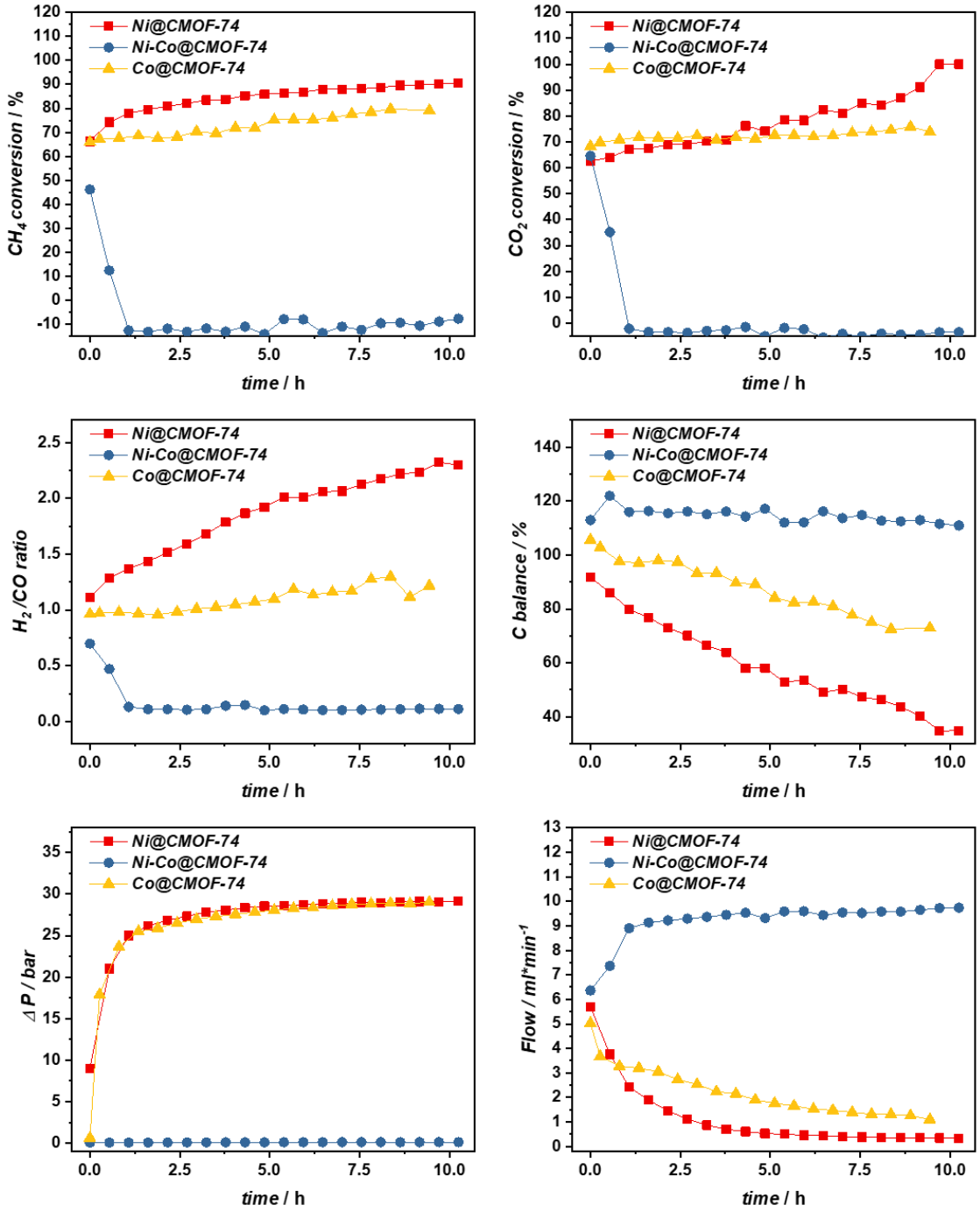

Figure S10. Catalytic results of the different M@CMOF-74 catalysts at 750 °C, 5 bar, 63 $L*h^{-1}*g^{-1}$.

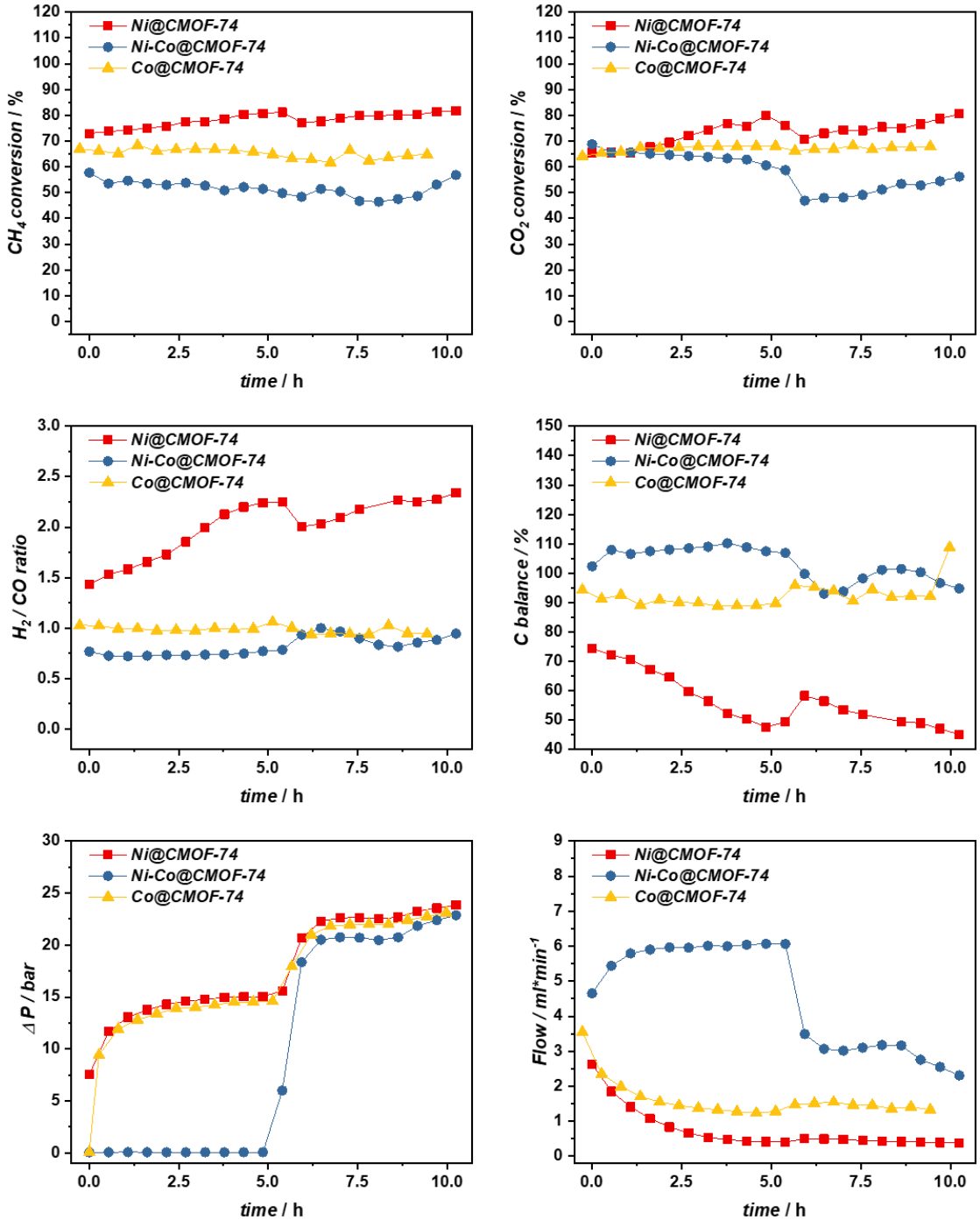

Figure S11. Catalytic results of the different M@CMOF-74 catalysts at 750 °C, 10 bar, 33 $L*h^{-1}*g^{-1}$.

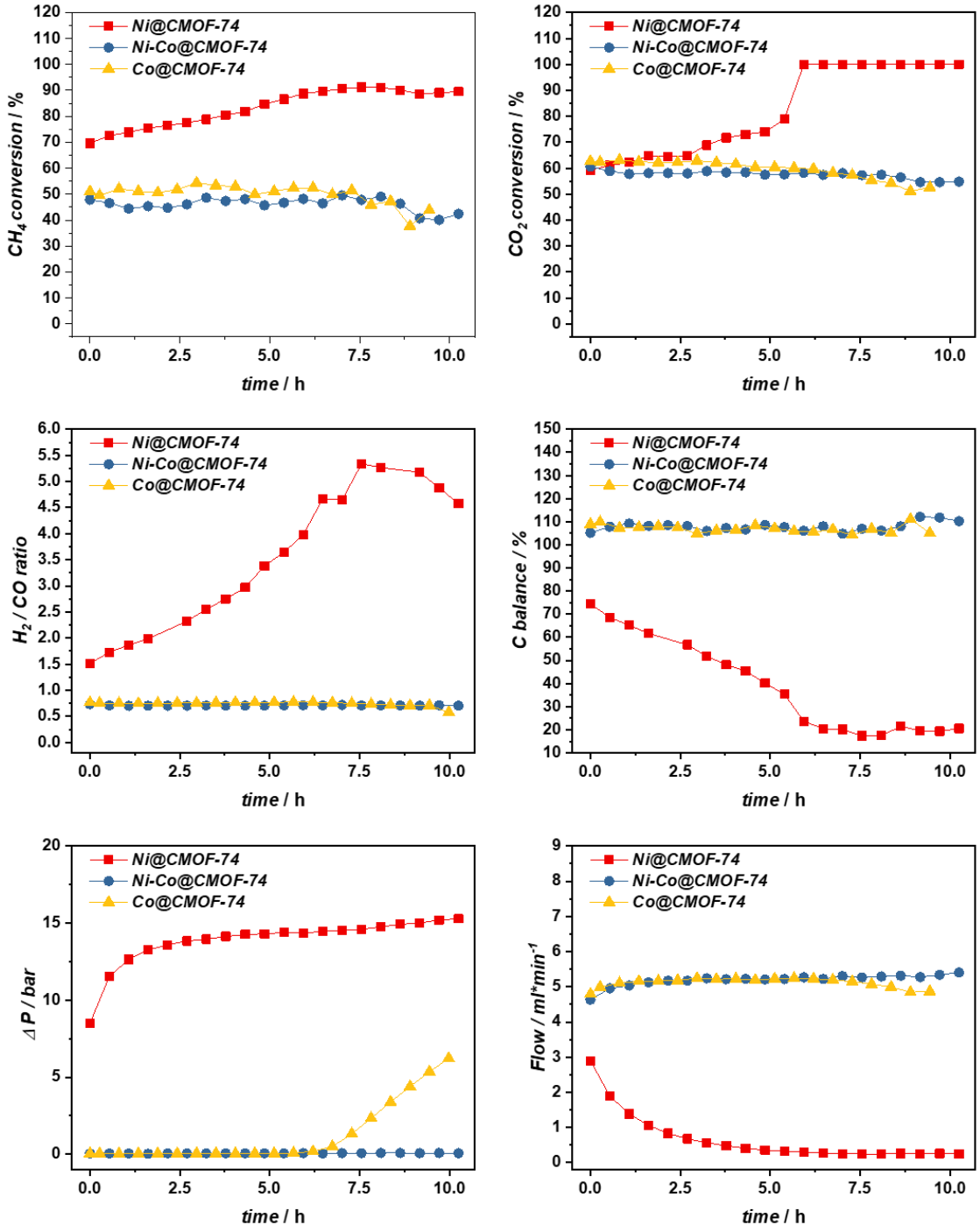

Figure S12. Catalytic results of the different M@CMOF-74 catalysts at 700 °C, 5 bar, 33 $L*h^{-1}*g^{-1}$.

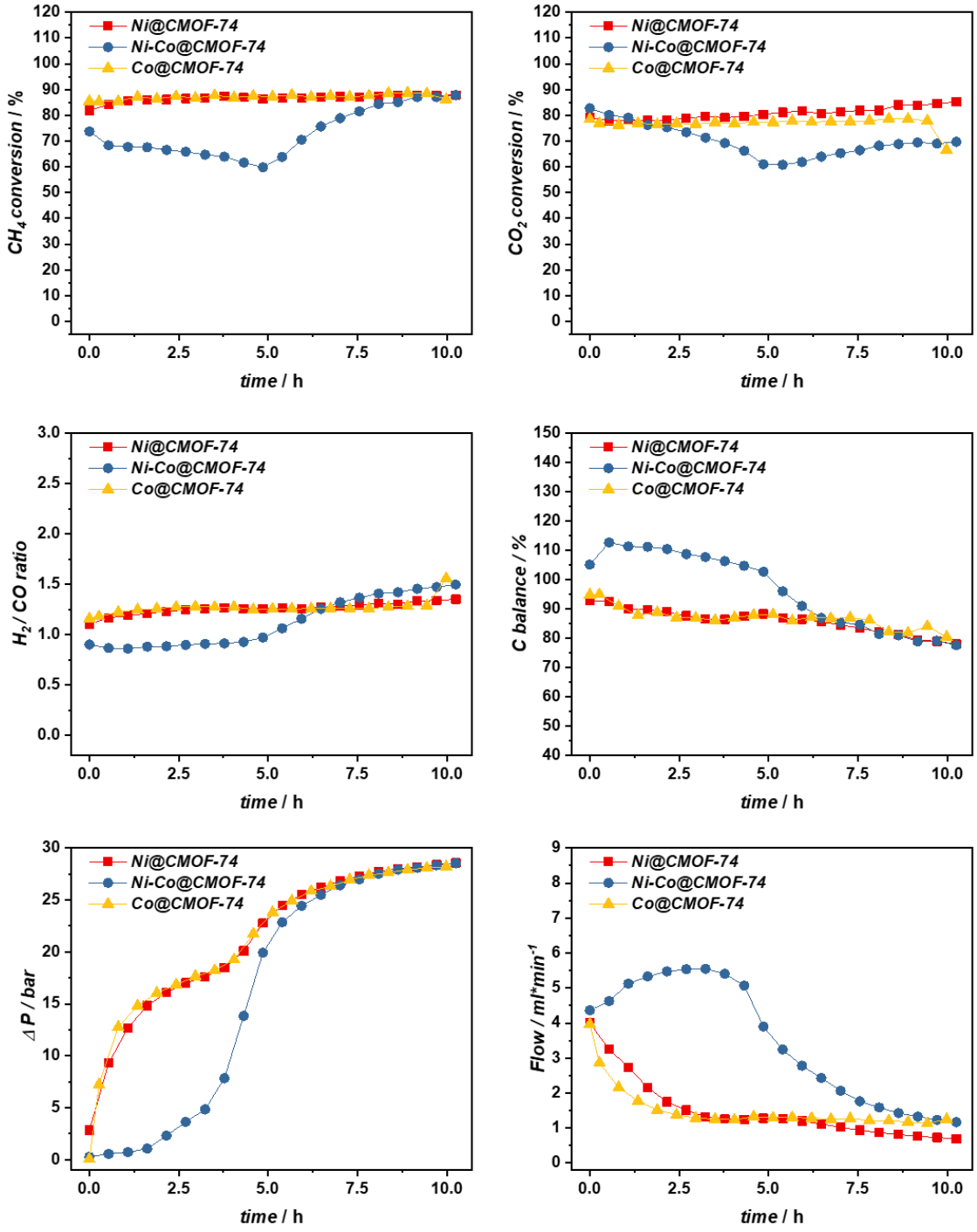

Figure S13. Catalytic results of the different M@CMOF-74 catalysts at 800 °C, 5 bar, 33 $L*h^{-1}*g^{-1}$.

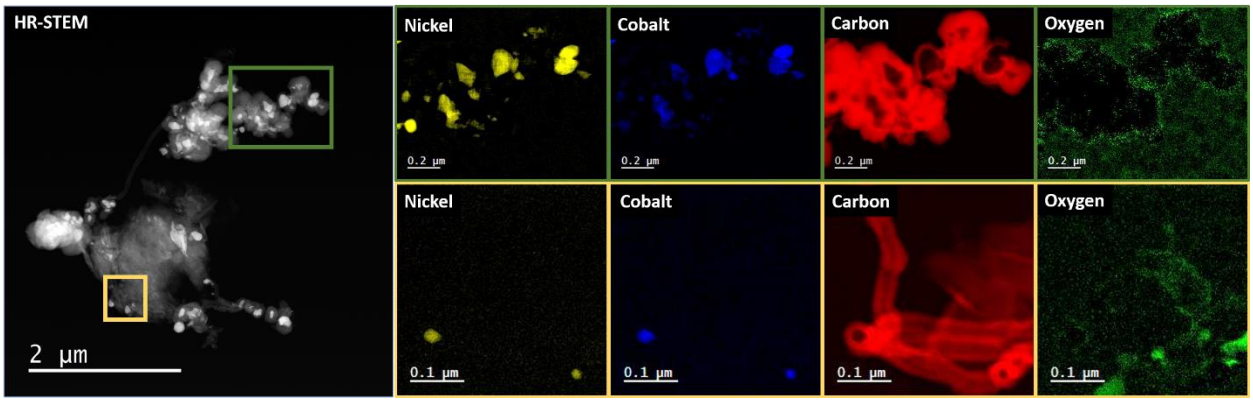

Figure S14. High-resolution dark field STEM images of spent Ni-Co@CMOF-74 catalyst and STEM-EELS mapping showing the distribution of Ni (yellow), Co (blue), C (red) and O (green) throughout the solid after 10 hours of reaction. Reaction condition: 750 °C, 5 bar and 33 $L*h^{-1}*g^{-1}$.

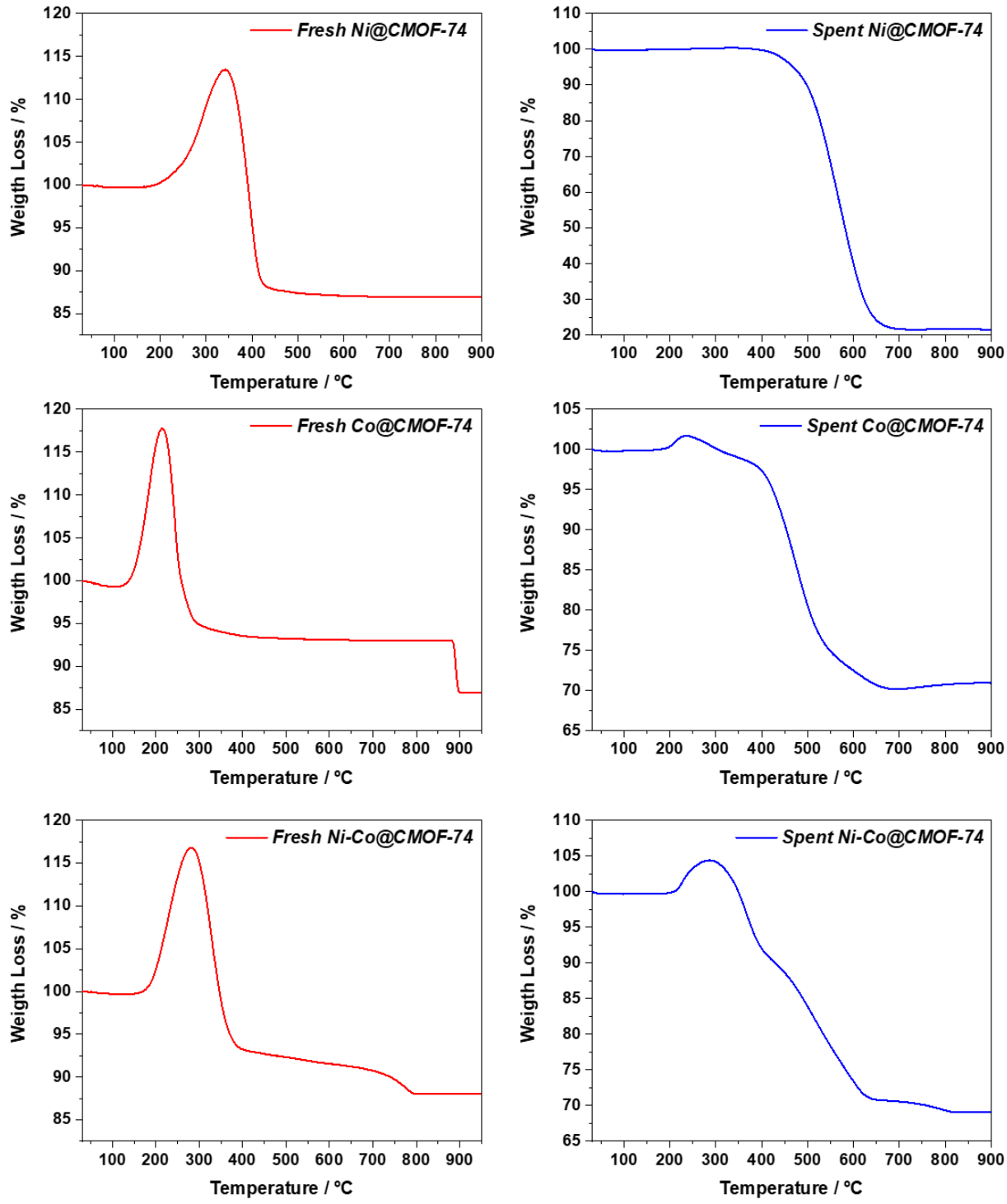

Figure S15. Thermogravimetric curves for the fresh (left) and spent (right) M@CMOF-74 catalysts in air.

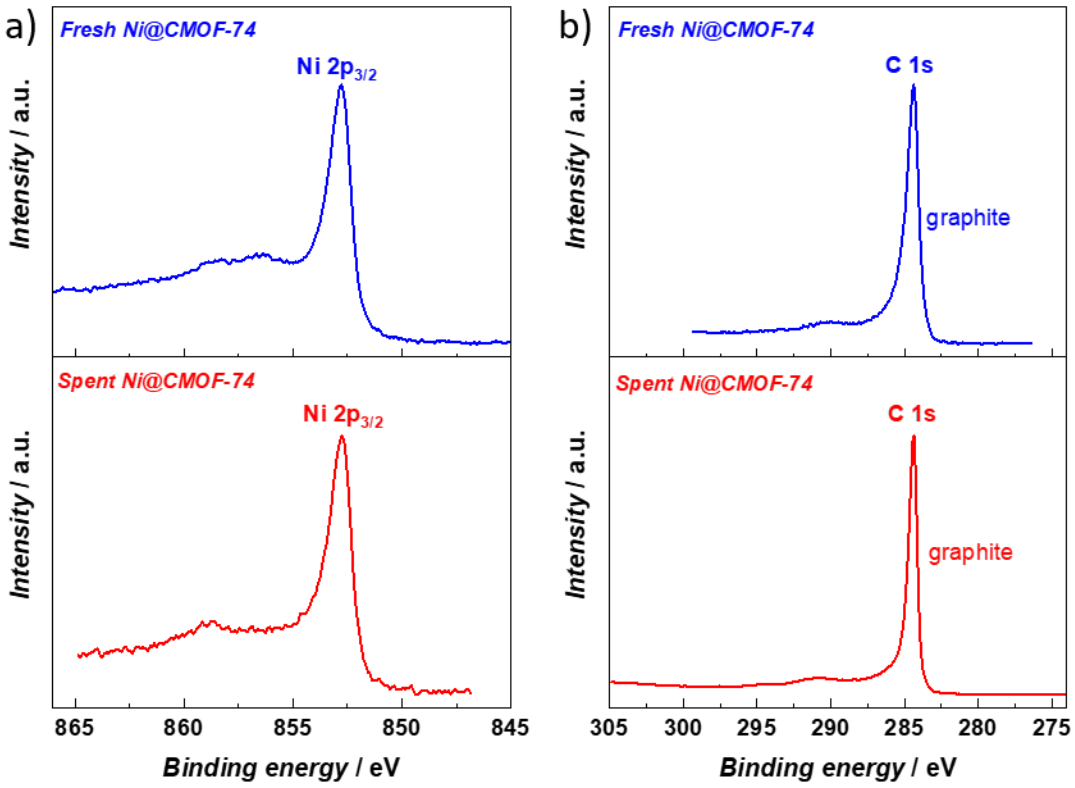

Figure S16. X-ray photoelectron spectroscopy of the Ni@CMOF-74 solid before and after reaction with core levels a) Ni(2p) and b) C(1s).

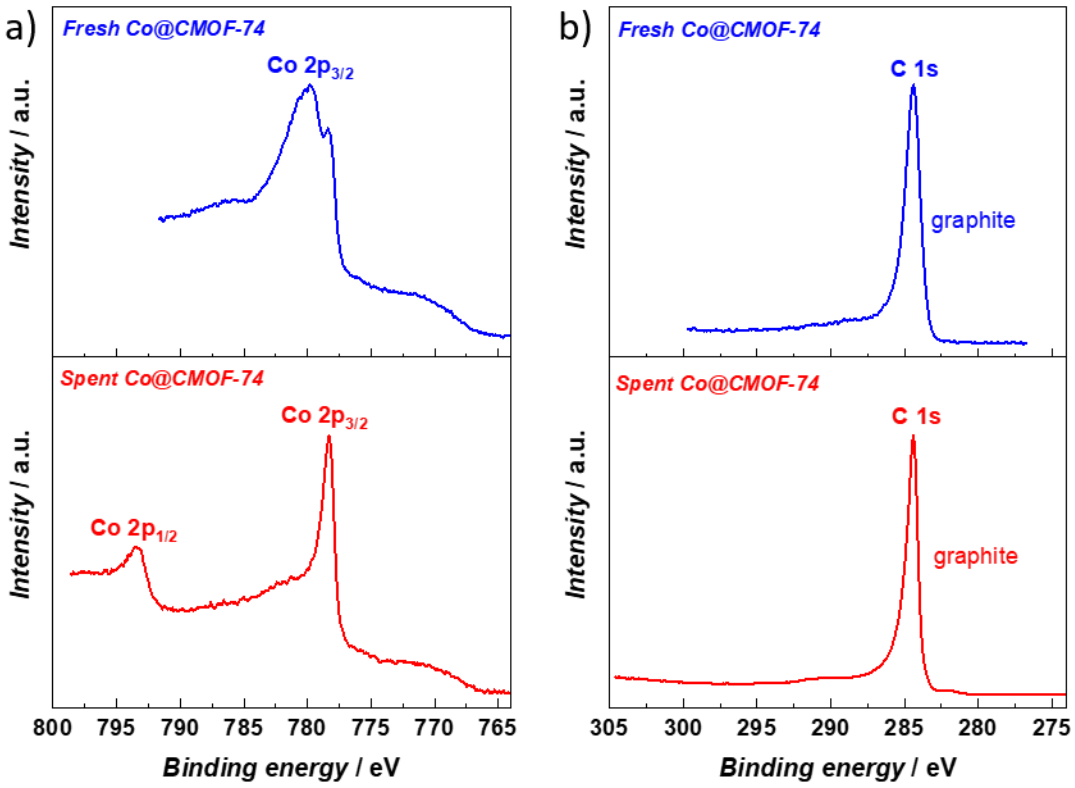

Figure S17. X-ray photoelectron spectroscopy of the Co@CMOF-74 solid before and after reaction with core levels a) Co(2p) and b) C(1s).

Table S1. Comparison of Carbon supported materials for the DRM reported in literature with the Ni-Co@CMOF-74 catalyst.

Catalyst	Temperature (°C)	Pressure (bar)	CH_4 conversion	CO_2 conversion	CH_4/CO_2	TOS* (hours)	Ref.
I-Ni/CNTs	700	1	55	67	1	8	[1]
O-Ni/CNTs	700	1	50	57	1	8	[1]
Ni/AC	700	1	45	51	1	8	[1]
Co/AC	700	1	75	50	1	5	[2]
AC	700	1	3	7	1	1	[3]
AC-$NaNO_3$	700	1	18	30	1	1	[3]
Ni-Co@CMOF-74	700	5	49	58	1	10	This work
I-Ni/CNTs	750	1	71	83	1	8	[1]
O-Ni/CNTs	750	1	60	75	1	8	[1]
Ni/AC	750	1	50	67	1	8	[1]
Co/AC	750	1	78	67	1	5	[2]
AC	750	1	18	25	1	1	[3]
Ni-Co@CMOF-74	750	5	60	69	1	10	This work

*Time till deactivation

References

1. Ma, Q.; Wang, D.; Wu, M.; Zhao, T.; Yoneyama, Y.; Tsubaki, N. Effect of catalytic site position: Nickel nanocatalyst selectively loaded inside or outside carbon nanotubes for methane dry reforming. *Fuel* **2013**, *108*, 430–438, https://doi.org/10.1016/j.fuel.2012.12.028.
2. Zhang, G.; Su, A.; Du, Y.; Qu, J.; Xu, Y. Catalytic performance of activated carbon supported cobalt catalyst for CO2 reforming of CH4. *J. Colloid Interface Sci. Science* **2014**, *433*, 149–155, https://doi.org/10.1016/j.jcis.2014.06.038.
3. Xu, L.; Liu, Y.; Li, Y.; Lin, Z.; Ma, X.; Zhang, Y.; Argyle, M.D.; Fan, M. Catalytic CH4 reforming with CO2 over activated carbon based catalysts. *Appl. Catal., A* **2014**, *469*, 387–397, https://doi.org/10.1016/j.apcata.2013.10.022.